Dynamic selective switching in antiferromagnetically-coupled bilayers close to the spin reorientation transition

A. Fernández-Pacheco, F. C. Ummelen, R. Mansell, D. Petit, J. H. Lee, H. J. M. Swagten, and R. P. Cowburn

Citation: Applied Physics Letters **105**, 092408 (2014); doi: 10.1063/1.4895032
View online: http://dx.doi.org/10.1063/1.4895032
View Table of Contents: http://scitation.aip.org/content/aip/journal/apl/105/9?ver=pdfcov
Published by the AIP Publishing

Dynamic selective switching in antiferromagnetically-coupled bilayers close to the spin reorientation transition

A. Fernández-Pacheco,[1,a)] F. C. Ummelen,[2] R. Mansell,[1] D. Petit,[1] J. H. Lee,[1] H. J. M. Swagten,[2] and R. P. Cowburn[1]
[1]*Cavendish Laboratory, University of Cambridge, J. J. Thomson Avenue, Cambridge CB3 0HE, United Kingdom*
[2]*Department of Applied Physics, Center for NanoMaterials, Eindhoven University of Technology, P.O. Box 513, 5600 MB Eindhoven, The Netherlands*

(Received 23 July 2014; accepted 26 August 2014; published online 5 September 2014)

We have designed a bilayer synthetic antiferromagnet where the order of layer reversal can be selected by varying the sweep rate of the applied magnetic field. The system is formed by two ultra-thin ferromagnetic layers with different proximities to the spin reorientation transition, coupled antiferromagnetically using Ruderman-Kittel-Kasuya-Yosida interactions. The different dynamic magnetic reversal behavior of both layers produces a crossover in their switching fields for field rates in the kOe/s range. This effect is due to the different effective anisotropy of both layers, added to an appropriate asymmetric antiferromagnetic coupling between them. Field-rate controlled selective switching of perpendicular magnetic anisotropy layers as shown here can be exploited in sensing and memory applications. © *2014 AIP Publishing LLC*.
[http://dx.doi.org/10.1063/1.4895032]

Synthetic antiferromagnets (SAFs) formed by two ferromagnetic layers coupled antiferromagnetically using Ruderman-Kittel-Kasuya-Yosida (RKKY) interactions are currently used in technologically relevant systems such as magnetic random access memories (MRAMs) or spin-valve Giant Magnetoresistance (GMR) heads.[1–3] Traditionally, these systems have been formed by in-plane (IP) materials with the anisotropy arising from the shape of patterned structures.[2] Aiming to move towards higher densities, IP materials are being substituted by films with high perpendicular magnetic anisotropy (PMA), which have high thermal stability and sharp magnetic switching.[2–4] Recently, in order to reduce the critical current density of spin-transfer-torque MRAM, alternative magnetic systems which combine IP and PMA materials have been proposed.[2,3] Furthermore, systems where the magnetization of one of the magnetic electrodes is canted, forming non-collinear magnetic configurations between layers, should reduce substantially the writing energy of these devices.[5–7] These last systems can be realized using asymmetric SAFs, where fine control of the effective anisotropy of the layers and the coupling between them is required.[8,9] For the implementation of non-collinear bilayers into devices, it is essential to understand in detail their magnetic properties. In particular, the dynamic behavior of PMA layers can be very different depending on their effective anisotropy, changing their reversal mechanisms and coercivity as a function of the field sweep rate (dH/dt).[10–12] In symmetric or low-asymmetry SAFs, the dH/dt dependence of the switching fields will be similar for both films, implying that the order of reversal of the films will be always the same, irrespective of how fast the field is applied. In this letter, we study a highly-asymmetric SAF formed by two ferromagnetic layers with different proximity to the spin-reorientation transition (SRT), i.e., with very different effective anisotropy values. As a consequence, the magnetization reversal mechanisms for both layers are different, which results in substantially different dependences of the coercive field with dH/dt. This, together with an appropriate antiferromagnetic coupling between layers, results in a crossover of the switching fields of the two layers in the kOe/s range, which makes possible to select which of the two layers will switch first by applying a field either faster or slower than the value where this crossover is produced.

The samples were grown by magnetron sputtering, with a base pressure of 5×10^{-8} millibar and a growth pressure of 10^{-2} millibar. Magnetic switching was studied at different dH/dt using a focused magneto-optical Kerr effect (MOKE) system, applying ac magnetic fields of up to ~1 kOe with varying frequencies between 0.01 Hz and 20 Hz. Magnetic domains during switching were imaged using the same MOKE system by scanning laser Kerr microscopy, with a laser spot of ~5 μm. Figs. 1(a)–1(d) show low field sweep rates (3,650 Oe/s) polar MOKE hysteresis loops corresponding to the switching of Co single layers [Ta(4 nm)/Pt(10 nm)/Co(t)/Pt(2 nm)/Ta(2 nm)] of varying thickness t = 0.8–2 nm, as indicated in the figure. Figs. 1(e)–1(h) are corresponding Kerr images obtained during the switching of the layers. The SRT occurs at $t_c \approx 2$ nm, for which $K_{eff} = K_d + K_{PMA} = 0$, where $K_d = -2\pi M_s^2$ is the demagnetizing anisotropy and $K_{PMA} = 2K_s/t$ is the PMA energy density. This corresponds to a surface anisotropy $K_s = 1.2$ erg/cm^2 for Co, with the saturation magnetization assumed to be $M_s = 1400$ emu/cm^3, and neglecting second order anisotropy terms. For films with $0.4\text{ nm} < t < 0.9\text{ nm}$, K_{PMA} is much higher than K_d, with the magnetization switching sharply via thermally-activated propagation of only a few domains (Fig. 1(e)). The films show full remanence with the coercive field determined by defects in the film;[10] in these cobalt samples, $H_c \approx 425$ Oe at 1.9 kOe/s. For $0.8\text{ nm} < t < 1.9\text{ nm}$, K_{PMA} approaches K_d, the domains are more numerous, reduce in size, and show more

a)af457@cam.ac.uk

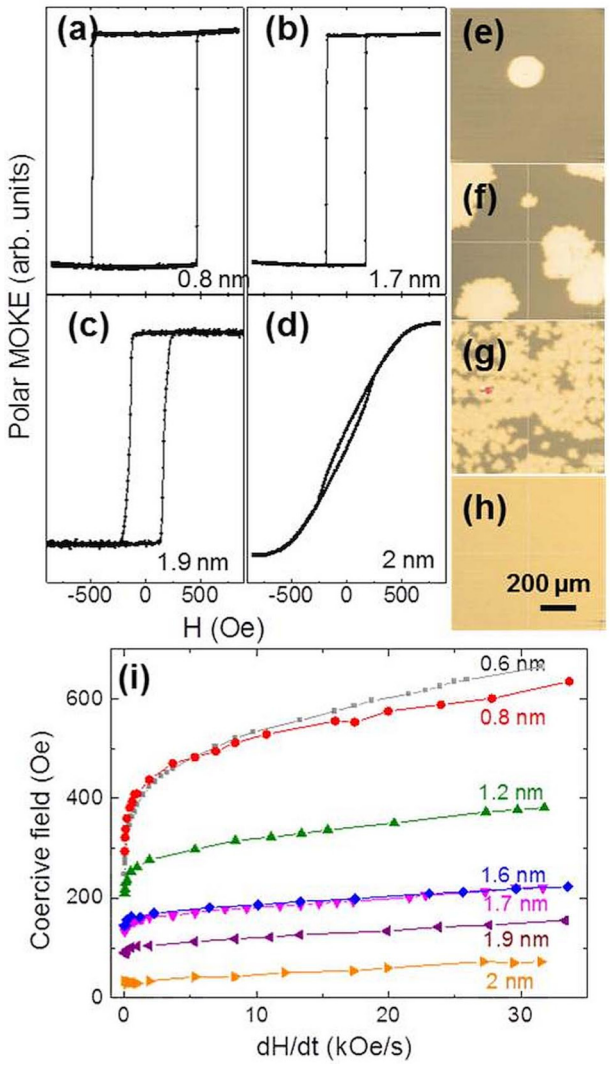

FIG. 1. (a)–(d) Polar hysteresis loops of Pt/Co(t)/Pt films near the SRT. The thickness t of the Co layers is indicated in the inset. All loops are recorded at field rates ≈ 3.65 kOe/s. (e)–(h) Polar Kerr microscopy images of those layers during magnetization reversal. (i) Coercive field dependence of the films as a function of the field sweep rate.

jagged edges, due to the reduction in anisotropy and the non-negligible effect of dipolar interactions.[10] The reversal here is dominated by thermally-activated nucleation processes, with a significant reduction in coercivity and reduced remanence. For t = 2 nm, a hard axis loop is observed, with a low saturation field (~500 Oe), as expected for a film just thicker than t_c.[13] The switching of this layer occurs mostly via coherent rotation of the magnetization. The small hysteresis loop observed is due either to field misalignment or to a small number of out-of-plane domains likely caused by small thickness variations along the sample. These domains are not observed in the Kerr images during reversal (only the image at remanence is shown here—Fig. 1(h)), which indicates that they are smaller than our Kerr microscope resolution (~5 μm). In summary, coercive fields, domain structure, and magnetization reversal mechanism depend critically on film thickness close to the SRT, due to the large changes in K_{eff} for this thickness range.[10,13]

We show the magnetization reversal dynamics of the samples through the sweep rate dependent coercivity in Fig. 1(i). The coercive fields increase as a function of field sweep rate, as expected for thermally-activated mechanisms,[14] but in a very different manner depending on the layer thickness. It is well-established that whereas H_c will approximately vary as ln(dH/dt) for propagation-dominated processes,[10] the behavior is more complex for nucleation-dominated ones,[11] with the variation of H_c with dH/dt becoming more moderate.[15] The different dynamical behavior with thickness observed in Fig. 1(i) is due to the following: Thicker films (for instance t = 1.9 nm) present a shallow increase of H_c with dH/dt for all the field sweep range studied, since the reversal is nucleation-dominated for all frequencies. On the contrary, two different regions are observed for thinner films (see for instance t = 0.8 nm): at low rates (dH/dt < 5 kOe/s), a sharp increase of H_c with dH/dt is observed, as the magnetization reversal is propagation-dominated. At higher rates, however, a more moderate increase of H_c with dH/dt is again observed. In that range, the reversal becomes nucleation-dominated, as the field rate becomes faster than the domain propagation speed, which fosters the formation of multiple domains. The graph includes the variation of H_c with dH/dt for the thickest film studied, i.e., t = 2 nm, just at the edge of the SRT, with a similar behavior as the one present for films just slightly thinner. This coercivity corresponds to the one present in hard-axis like loops as the one shown in Fig. 1(d) and previously discussed. For the saturation field of these loops, no change with field speed is observed, as expected for reversal via coherent rotation of the magnetization.[16]

We have exploited the differences in dynamic reversal properties as a function of film thickness to create a SAF with variable switching order, controlled via the field sweep rate. The system consists of two antiferromagnetically-coupled layers, Co and CoFeB, with different thicknesses: Ta(4)/Pt(10)/Co(2)/Pt(0.7)/Ru(0.9)/Pt(0.7)/CoFeB(1)/Pt(2)/Ta(2). Ru thickness is chosen at the first antiferromagnetic peak, and the two Pt layers at the Ru interfaces both favor the PMA of the films and control the AF coupling between layers.[17] The thickness for Co and CoFeB layer is chosen to obtain very different dynamic switching behaviors: Co (2 nm), as previously discussed, is just at the edge of the SRT, where coercivity has a very mild dependence with field speeds. On the contrary, CoFeB (1 nm) is much thinner than the SRT critical thickness (t_c = 1.6 nm for CoFeB, not shown here), and has a similar behavior as the thinnest Co films previously discussed. Figs. 2(a)–2(c) show single-shot hysteresis loops of this bilayer system for three different field sweep rates. Remarkably, the switching order of the bilayer system depends on the value of dH/dt. Whereas, at low field speeds (Fig. 2(a)), coming from saturation, an abrupt switch is observed first, corresponding to the CoFeB layer, the contrary occurs for high field speeds (Fig. 2(c)), where a slanted transition corresponding to Co switching happens before. The arrows in the inset sketch the resulting state coming from negative saturation after the first switching, where the top (blue) arrows correspond to CoFeB and the bottom (black) to Co. Therefore, these two graphs show how the system can be remotely addressed via ac fields: for low field rates, the top CoFeB layer becomes anti-parallel to the previous saturation field, whereas at high rates, this layer stays parallel. Fig. 2(b) shows a typical single-shot hysteresis loop for intermediate field rates, where the switching is not deterministic anymore, which can result into asymmetric

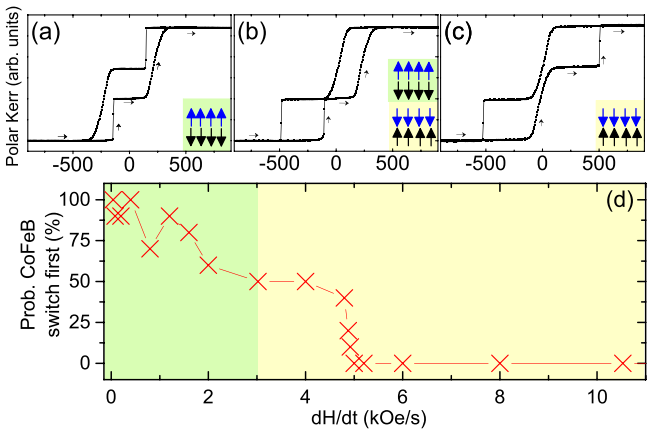

FIG. 2. (a)–(c) Polar hysteresis loops at three different field rates of a Pt/Co(2 nm)/Pt/Ru/Pt/CoFeB(1 nm)/Pt SAF. The arrows in the inset show the state of the system coming from negative saturation, which depends on the field rate. The loops correspond to 240 Oe/s (a), 2.3 kOe/s (b), and 10.6 kOe/s (c). (d) Probability that the Pt/CoFeB/Pt layer will switch before from saturation, calculated from 10 independent events. A crossover from CoFeB switching first to Co switching first is observed at ≈3 kOe/s. The figure background is colored in green and yellow for both regions, and the same color scheme is used in Figure 3 to help the reader to interpret the results.

switching as observed in the figure: coming from negative saturation CoFeB switches first, and coming from positive saturation Co switches first. Different single-shot Kerr loops (not shown here) show different possible switching orders, i.e., in other cases, either CoFeB (Co) always switches first for both branches or the loop asymmetry is the contrary to the one shown here. How frequently one or other behavior is observed is field sweep dependent, as illustrated in Fig. 2(d), where the probability of CoFeB switching first as a function of field sweep rate, calculated from 10 events, is shown. At very low field speeds, there is a 100% probability of CoFeB switching before Co, whereas it becomes zero at $dH/dt > 5$ kOe/s. 50% probability value is observed for $dH/dt \sim 3$ kOe/s. In order to observe this non-deterministic intermediate switching regime, the maximum field applied is set at ~1.2 kOe. This guarantees that both layers are fully saturated at the maximum field, with no nucleation embryos present at saturation.[18] On the contrary, if the maximum field is set to smaller values (not shown here), we observe that the switching order becomes deterministic at intermediate dH/dt values, an indication that the switching is dominated in this case by remaining unsaturated nucleation embryos.

In order to achieve variable switching order, we have used the different coercivity dependences that layers with different proximity to the SRT have. However, a film very close to the SRT, with small dependence for H_c with dH/dt, presents very low coercivity values, in general, always smaller than a thinner film far from the SRT, which is the one with a large variation of H_c with dH/dt. The crossover in switching fields observed in this asymmetric SAF is only possible due to the different coupling fields of the two layers. In a bilayer such as the one studied, formed by two ferromagnetic layers anti-ferromagnetically coupled by a metallic spacer via RKKY interactions, the switching field for each layer is determined by its coercivity H_{ci} and inter-layer coupling field $H_{Ji} = |J|/t_i M_{si}$, where J is the inter-layer coupling surface energy density in erg/cm^2, t the layer thickness and M_s the saturation magnetization. From negative-to-positive saturation and using an Ising approximation, the switching fields from parallel (P) to anti-parallel (AP) configuration, and vice versa, are $H_{swi}(P \rightarrow AP) = H_{ci} - H_{Ji}$ and $H_{swi}(AP \rightarrow P) = H_{ci} + H_{Ji}$.

Fig. 3(a) shows the field sweep rate dependence for both switching fields, calculated for single layers with thicknesses equal to those forming the bilayer under study, and as if they were forming a ("virtual") bilayer system as the one studied here. Circles (squares and triangles) show switching fields for CoFeB (Co), and open (full) symbols correspond to $H_{swi}(AP \rightarrow P)$ ($H_{swi}(P \rightarrow AP)$). These switching fields have been calculated using the experimental H_{ci} measured for single layers and the two different H_{Ji} obtained from analyzing the bilayer system under study, as explained below. In particular, the figure shows data for a 1 nm-thick CoFeB layer [Ta(4)/Pt(10)/CoFeB(1)/Pt(2)/Ta(2)] and two Co layers [Ta(4)/Pt(10)/Co(x)/Pt(2)/Ta(2)], with x = 1.9 and 2 nm. Although the Co thickness of the film forming the bilayer system is nominally 2 nm, we compare its behavior with two different Co single layers with thicknesses just before and after the SRT. Sub-nm range variations are expected between and within samples, and the behavior of these two layers is very different. Fig. 3(b) shows the corresponding switching fields for the ("real") bilayer, experimentally measured as a function of dH/dt. As the determination of the switching fields for Co is ambiguous, since the transitions of this layer are slanted, the values shown in the graph correspond to the field half way through the transition. This is not an issue for CoFeB, which presents well-defined sharp transitions. At low field rates, as previously explained, CoFeB switches first from $P \rightarrow AP$, followed by Co from $AP \rightarrow P$ for higher fields, with the contrary scenario for high rates. For the intermediate dH/dt range, where both options are possible, the figure plots the most probable situation. From these data, the coupling fields H_{Ji} for each layer can be estimated, as indicated in the graph, corresponding to $H_{J1} = 290$ Oe for CoFeB and $H_{J2} = 135$ Oe for Co. A common coupling surface energy density $|J| = 36 \pm 3$ merg/cm^2 is obtained, in good agreement with the one determined using minor loops (not shown here). The values extracted for H_{Ji} have been used to calculate H_{swi} in the virtual bilayer in order to compare it with the real one, and assess the validity of the analysis carried out here.

We should note that this analysis involves several simplifications: The values of the coercivity of the single layers

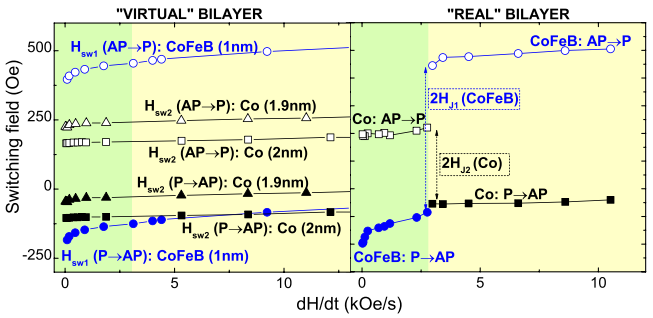

FIG. 3. Switching fields of the "virtual" (a) and "real" (b) bilayer as a function of field sweep rate, including P→AP and AP→P transitions. In (b), coupling fields determined for both layers are indicated by dashed arrows.

and of the films forming the bilayer will differ between them slightly, since they were grown in different growth processes (and on top of different under-layers in the case of the CoFeB film). Moreover, the coupling field of both layers has been extracted using an Ising approximation, whereas the reversal of the Co layer is far from being Ising-like; the exact configuration and reversal process of this layer is complex, characterization of which will be published elsewhere. Last, any possible effect of the coupling on the coercivity of the films is not taking into account in the virtual bilayer: Here the coupling is considered merely as a field shifting the coercivity of single layers; possible binding effects during the reversal of the real bilayer due to the coupling field coming from RKKY interactions[19] have not been considered. In spite of those simplifications, a quite good agreement is observed between the switching fields experimentally determined in the virtual and in the real bilayer using this analysis (comparison of Figs. 3(a) and 3(b)).

It is particularly interesting to analyze the P → AP transition for the virtual bilayer (Fig. 3(a)) and its dependence with dH/dt for the different range values. For low field rates, H_{sw1} is significantly more negative than H_{sw2}, implying that the CoFeB layer will switch first, as observed in the real bilayer (Fig. 3(b)). For the range where the crossover in switching fields occurs (marked by a color change in the figures, corresponding to ∼3 kOe/s), the asymmetric coupling for both layers result in H_{sw1} and H_{sw2} approaching closely. A crossover should be then observed, with H_{sw2} becoming more negative than H_{sw1} since Co should switch first from that field onwards. No crossover, however, occurs for this range, but at larger dH/dt (∼7 kOe/s) if the 2 nm Co film is considered, and it does not crossover at all if the 1.9 nm Co film is considered instead. For higher dH/dt values, the H_{sw2} values and those for the real bilayer are quite similar, especially for the 1.9 nm-thick Co film. The discrepancy at the range where the crossover occurs, shows that the behavior in the real bilayer is, indeed, more complex than the model followed here. In particular, the P→AP switching field of the CoFeB film in the real bilayer (Fig. 3(b)) has a remarkably more abrupt evolution with dH/dt at the crossover range than the CoFeB single layer. This suggests that binding effects between layers[19] are especially important for these dH/dt values, where both layers are likely to switch. In spite of this disagreement, the simple model presented here gives account of many of the features observed in the bilayer, constituting a good starting point to select what values for film thicknesses and RKKY coupling are needed in order to design SAFs with dynamic selective switching. If a different coupling strength value, J, was chosen, the range of field rates where the crossover occurs would be shifted, constituting a way to tune the operating range of this device. It should be, however, noted that the use of much larger couplings is expected to lead to different switching behaviors from those shown here: The layers will reverse via flopping, binding effects between them will be modified, and the two possible anti-parallel states of the system could be present in a major loop.[20] Finally, we should remark that the effect studied here will only occur in SAFs formed by two layers with (different) thicknesses close to the SRT, since a net coupling field between layers is required. Ultra-thin films with strong PMA and thick films where the magnetization is purely in plane also have significantly different dynamic switching field dependences;[11,13] however, in a SAF formed by these two types of layers and under uniaxial coupling, selective dynamic switching as the one studied in this work will not be possible, since the system will present zero inter-layer coupling as the magnetization of the layers will lie at 90 degrees from each other.

In conclusion, we have designed a highly-asymmetric synthetic antiferromagnet formed by two ultra-thin Pt/Co/Pt and Pt/CoFeB/Pt ferromagnetic layers coupled via Ru using RKKY interactions, where the switching order of the films can be selected by controlling the field sweep rate. The combination of two layers with different proximities to the spin reorientation transition and an appropriate coupling value between layers makes possible this effect. Dynamic field-controlled remote addressing of asymmetric synthetic antiferromagnets as shown here may find applications in sensing and storage technologies where devices sensitive to the speed of an applied external magnetic field are required. Here, we have studied a system where the field sweep rate occurs in the range of a few kOe/s. The use of different materials with higher domain velocities,[21] the possibility to control the switching dependence of the material via doping,[22] or by applying electric fields[23] may extend this effect at different field rates and in a tunable manner.

This work was funded by the European Community under the Seventh Framework Programme Contract No. 247368: 3SPIN, and by a European Erasmus Mobility program.

[1]C. Chappert, A. Fert, and F. N. Van Dau, Nat. Mater. **6**, 813 (2007).
[2]A. V. Khvalkovskiy, D. Apalkov, S. Watts, R. Chepulskii, R. S. Beach, A. Ong, X. Tang, A. Driskill-Smith, W. H. Butler, and P. B. Visscher, J. Phys. D: Appl. Phys. **46**, 074001 (2013).
[3]K. L. Wang and P. K. Amiri, SPIN **2**, 1250009 (2012).
[4]S. Ikeda, K. Miura, H. Yamamoto, K. Mizunuma, H. D. Gan, M. Endo, S. Kanai, J. Hayakawa, F. Matsukura, and H. Ohno, Nat. Mater. **9**, 721 (2010).
[5]R. Sbiaa, R. Law, E.-L. Tan, and T. Liew, J. Appl. Phys. **105**, 013910 (2009).
[6]C.-Y. You, Appl. Phys. Lett. **100**, 252413 (2012).
[7]C.-Y. You, J. Appl. Phys. **115**, 043914 (2014).
[8]J. Choi, B.-C. Min, J.-Y. Kim, B.-G. Park, J. H. Park, Y. S. Lee, and K.-H. Shin, Appl. Phys. Lett. **99**, 102503 (2011).
[9]W. Kuch, X. Gao, and J. Kirschner, Phys. Rev. B **65**, 064406 (2002).
[10]J. Ferré, *Spin Dynamics in Confined Magnetic Structures I*, Topics in Applied Physics Vol. 83, edited by B. Hillebrands and K. Ounadjela (Springer, 2002), pp. 127–168.
[11]B. Raquet, R. Mamy, and J. C. Ousset, Phys. Rev. B **54**, 4128 (1996).
[12]T. A. Moore and J. A. C. Bland, J. Phys.: Condens. Matter **16**, R1369 (2004).
[13]M. Kisielewski, A. Maziewski, M. Tekielak, J. Ferré, S. Lemerle, V. Mathet, and C. Chappert, J. Magn. Magn. Mater. **260**, 231 (2003).
[14]G. Malinowski, S. van Dijken, M. Czapkiewicz, and T. Stobiecki, Appl. Phys. Lett. **90**, 082501 (2007).
[15]Some results presented in the literature plot H_c as a function of dH/dt with the x-axis in a logarithmic scale, which can give the false impression that the rate of change of H_c is larger at high field rates than at low ones. A linear scale plot as the one shown makes clear that H_c changes faster for low dH/dt values.
[16]J. Vogel, J. Moritz, and O. Fruchart, C. R. Phys. **7**, 977 (2006).
[17]R. Lavrijsen, A. Fernández-Pacheco, D. Petit, R. Mansell, J. H. Lee, and R. P. Cowburn, Appl. Phys. Lett. **100**, 052411 (2012).

[18]Y. L. Iunin, Y. P. Kabanov, V. I. Nikitenko, X. M. Cheng, D. Clarke, O. A. Tretiakov, O. Tchernyshyov, A. J. Shapiro, R. D. Shull, and C. L. Chien, Phys. Rev. Lett. **98**, 117204, (2007).
[19]P. J. Metaxas, R. L. Stamps, J.-P. Jamet, J. Ferré, V. Baltz, B. Rodmacq, and P. Politi, Phys. Rev. Lett. **104**, 237206 (2010).
[20]N. Wiese, T. Dimopoulos, M. Rührig, J. Wecker, and G. Reiss, J. Appl. Phys. **98**, 103904 (2005).
[21]K.-S. Ryu, L. Thomas, S.-H. Yang, and S. S. P. Parkin, Appl. Phys. Exp. **5**, 093006 (2012).
[22]R. Lavrijsen, G. Malinowski, J. H. Franken, J. T. Kohlhepp, H. J. M. Swagten, B. Koopmans, M. Czapkiewicz, and T. Stobiecki, Appl. Phys. Lett. **96**, 022501 (2010).
[23]D. Chiba, M. Kawaguchi, S. Fukami, N. Ishiwata, K. Shimamura, K. Kobayashi, and T. Ono, Nat. Commun. **3**, 888 (2012).